

Hippocampus-Associated Causal Network of Structural Covariance Measuring Structural Damage Progression in Temporal Lobe Epilepsy

Zhiqiang Zhang,^{1,2*} Wei Liao,^{1,3} Qiang Xu,¹ Wei Wei,¹
Helen Juan Zhou,⁴ Kangjian Sun,⁵ Fang Yang,⁶ Dante Mantini,⁷
Xueman Ji,¹ and Guangming Lu^{1,2*}

¹Department of Medical Imaging, Jinling Hospital, Nanjing University School of Medicine, Nanjing, 210002, China

²State Key Laboratory of Analytical Chemistry for Life Science, Nanjing University, Nanjing, 210093, China

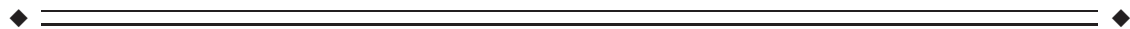
³Center for Cognition and Brain Disorders, Affiliated Hospital of Hangzhou Normal University, Hangzhou, 310015, China

⁴Center for Cognitive Neuroscience, Neuroscience and Behavioral Disorder Program, Duke-NUS Graduate Medical School, National University of Singapore, Singapore, Singapore

⁵Department of Neurosurgery, Jinling Hospital, Nanjing University School of Medicine, Nanjing, 210002, China

⁶Department of Neurology, Jinling Hospital, Nanjing University School of Medicine, Nanjing, 210002, China

⁷Faculty of Kinesiology and Rehabilitation Sciences, KU Leuven, Belgium



Abstract: In mesial temporal lobe epilepsy (mTLE), the causal relationship of morphometric alterations between hippocampus and the other regions, that is, how the hippocampal atrophy leads to progressive morphometric alterations in the epileptic network regions remains largely unclear. In this study, a causal network of structural covariance (CaSCN) was proposed to map the causal effects of hippocampal atrophy on the network-based morphometric alterations in mTLE. It was hypothesized that if cross-sectional morphometric MRI data could be attributed temporal information, for example, by sequencing the data according to disease progression information, GCA would be a feasible approach for constructing a CaSCN. Based on a large cohort of mTLE patients ($n = 108$), the hippocampus-associated CaSCN revealed that the hippocampus and the thalamus were prominent nodes exerting causal effects (i.e., GM reduction) on other regions and that the prefrontal cortex and cerebellum were prominent nodes being subject to causal effects. Intriguingly, compensatory increased gray matter volume in the contralateral temporal

Additional Supporting Information may be found in the online version of this article.

Contract grant sponsor: Natural Science Foundation of China; Contract grant number: 81422022, 81271553, 81401402, 81471653, 81201078 and 81201155; Contract grant sponsor: 863 project; Contract grant number: 2014BAI04B05 and 2015AA020505; Contract grant sponsor: China Postdoctoral Science Foundation; Contract grant number: 2013M532229; Contract grant sponsor: The Wellcome Trust; Contract grant number: 101253/Z/13/Z.

*Correspondence to: Zhiqiang Zhang; Department of Medical Imaging, Jinling Hospital, 305 Eastern Zhongshan Rd., Nanjing,

China, 210002. E-mail: zhangzq2001@126.com Guangming Lu; Department of Medical Imaging, Jinling Hospital, 305 Eastern Zhongshan Rd., Nanjing, China, 210002. E-mail: cjr.luguangming@vip.163.com

No statement of conflicts of interest.

Received for publication 23 December 2015; Revised 24 August 2016; Accepted 21 September 2016.

DOI: 10.1002/hbm.23415

Published online 28 September 2016 in Wiley Online Library (wileyonlinelibrary.com)

region and post cingulate cortex were also detected. The method unraveled richer information for mapping network atrophy in mTLE relative to the traditional methods of stage-specific comparisons and structured covariance network. This study provided new evidence on the network spread mechanism in terms of the causal influence of hippocampal atrophy on progressive brain structural alterations in mTLE. *Hum Brain Mapp* 38:753–766, 2017. © 2016 Wiley Periodicals, Inc.

Key words: temporal lobe epilepsy; progression; morphometric MRI; network of structural covariance; granger causality analysis

INTRODUCTION

Mesial temporal lobe epilepsy (mTLE) is the most common intractable type of human epilepsy. Hippocampal sclerosis (HS), as the usual pathological substrate of epileptogenic focus, and the limbic/temporal epileptic network engaging in propagation of epileptic activity, consist of the main physiopathologic basis of mTLE [Bartolomei et al., 2001; Spencer, 2002]. Moreover, mTLE associated with HS is firstly identified as a progressive disorder of epilepsy [Briellmann et al., 2002; Coan and Cendes, 2013; Fuerst et al., 2003]. Neuronal losses of hippocampus were correlated with disease durations and seizure incidences [Kalviainen et al., 1998; Tasch et al., 1999]. Propagation of seizure activity via temporal epileptic network also leads to progressive damages in the extra-hippocampal regions [Barron et al., 2014; Bartolomei et al., 2001; Bonilha and Halford, 2009; Keller et al., 2014; Moran et al., 2001; Sloviter, 1999; Spencer, 2002]. Investigation on the relationship of progressive brain damages between hippocampus and extra-extrahippocampal regions is essential for understanding the concept of epileptic network [Berg and Scheffer, 2011; Bonilha and Halford, 2009], and is also critical for clinical decision of mTLE management [Bernasconi and Bernhardt, 2010; Coan and Cendes, 2013; Pitkanen and Sutula, 2002].

Morphometric MRI has been the most favorable tool to study progression of structural damage of human brain in mTLE [Coan and Cendes, 2013]. Studies have revealed differential [Bernasconi et al., 2004, 2005; Bernhardt et al., 2013b; Bonilha et al., 2006] and related [Bonilha et al., 2003; Garcia-Finana et al., 2006; Goncalves Pereira et al., 2005; Mueller et al., 2010] atrophy in the hippocampus and extra-hippocampal regions (commonly including other

limbic structures, thalamus, frontal lobes, and cerebellum) in the epileptic network with progression of epilepsy, indicating the different roles and interactions of these structures in the pathogenesis of mTLE. Notably, a few of recent studies employed a structural covariance network (SCN) technique to delineate the synchronous GM atrophy among limbic and cortical regions, further mapped the topological pattern of network-reorganized regions in mTLE [Bernhardt et al., 2008; Bonilha et al., 2007; Duzel et al., 2006; Keller et al., 2014]. SCN employs correlation analysis for a cross-sectional morphometric imaging data, and measures synchronized GM atrophy undergoing common pathological processes between brain regions [Alexander-Bloch et al., 2013; Evans, 2013; Seeley et al., 2009]. However, correlation analysis is zero-time lagged, and cannot reflect temporal progression of neural incidences. Thus the topological patterns of progressive GM alterations in mTLE, in particular, the possible causal relationships of structural damages between epileptogenic focus of hippocampus and the other regions within the epileptic network remain largely unclear.

In analogy to correlation analysis used for time-series analysis, granger causality analysis (GCA) is another prevalent technique but it is time-dependent [Goebel et al., 2003; see also review: Seth et al., 2015]. Specifically, GCA can characterize brain information flow by detecting causal relation between two time-series. For utilization in functional data, Granger causal connectivity implicates that the neuronal activity in a region precedes and predicts the activity occurred in another region [Ji et al., 2013; Jiao et al., 2011; Palaniyappan et al., 2013]. Therefore, we hypothesized that if cross-sectional morphometric data can be given time-information, for example, by sequencing the cross-sectional data according to disease progression information, GCA would be a feasible approach for constructing a causal network of structural covariance (CaSCN).

CaSCN is assumed to allow mapping progressive alterations of structural brain network, and assessing the causal, in other words, temporal precedence relationship of morphometric alterations among network regions. In this study, based on morphometric data from a large cohort ($n = 108$) of mTLE patients, we constructed a hippocampus-associated CaSCN for mTLE. In contrast to the results from conventional methods of structural covariance network and stage-specific comparison, the CaSCN mapped the progressive

Abbreviations

CaSCN	causal network of structural covariance
GCA	granger causality analysis
GMV	gray-matter volume
HC	healthy controls
HS	hippocampal sclerosis
mTLE	mesial temporal lobe epilepsy
SCN	structural covariance network
VBM	voxel-based morphometry

profile of structural network organization in mTLE, and further assessed the causal influence of GM alterations among epileptogenic regions (hippocampus) and other network regions along with disease progression of mTLE.

MATERIALS AND METHODS

Participants

A total of 108 consecutive patients with unilateral (54 left- and 54 right-side) mTLE plus HS (gender: 56 males and 52 females; age: 27.6 ± 8.8 years) were recruited from Jinling hospital from June 2009 to September 2013. A portion of them had been reported in the previous publications [Ji et al., 2013]. MTLE was diagnosed through comprehensive evaluation including seizure history and semiology, neurological examination, diagnostic MRI, and EEG records. Unilateral HS was identified by conventional diagnostic MRI (atrophy of the hippocampus on coronal high-resolution T1 weighted images; high T2 signal on coronal FLAIR images and abnormal MR spectroscopy signal [Wu et al., 1998]). Exclusive criteria included: (i) Younger than 18 years, or older than 50 years. (ii) Other identifiable structural MRI abnormalities than the HS. (iii) Un-identified lateralization of mTLE. Among the patients, 61 patients had initial precipitating index (41 cases had history of febrile convulsion, and 20 cases had history of intracranial infections). Moreover, 48/88/89 patients presented symptoms of simple partial/complex partial/secondary generalized seizures. All patients had taken anti-epileptic drug medication (Valproate: $n = 61$; Carbamazepine: $n = 48$; Phenytoin: $n = 30$; Topiramate: $n = 21$; Oxcarbazepine: $n = 10$; Lamotrigine: $n = 8$; Phenobarbital: $n = 7$). Forty-seven patients had refractory epilepsy (resistance to more than two anti-epileptic drugs) and 42 patients underwent surgical treatment of anterior temporal lobectomy. Two clinical variables, epilepsy duration, and estimated number of lifetime seizures were used for describing the progression of epilepsy. Epilepsy duration was defined as time span from the onset time of habitual seizures to the scan time (11.2 ± 8.8 years) [Jokeit et al., 1997; Wei et al., 2016]. Estimated number of lifetime seizures was calculated by multiplying seizure frequency (5 times/day \sim 2 times/year, median: 3 times/month) with epilepsy duration, which is considered to be more comprehensive for depicting the damage level during disease progression (see also Supporting Information Fig. 1). The duration of epilepsy and seizure frequency was determined by interviewing the patient and at least one relative who lived in close contact with him/her. Patients were compared with 108 age- and gender-matched healthy controls (HCs) that were recruited from the staff of Jinling Hospital. This study was approved by the Medical Ethics Committee in Jinling Hospital, Nanjing University School of Medicine. Written informed consent was obtained from all the participants.

MRI Scans

MRI scans were conducted on a Siemens Magnetom Trio Tim 3T MR system. High resolution three-dimensional T1-weighted structural images were acquired with a fast spoiled gradient-echo sequence (FSPGR): repetition time/echo time/inversion time = 2,300 ms/2.98 ms/400 ms; Nex = 1; flip angle = 9° ; FOV = 256×256 cm²; matrix size = 256×256 ; slice thickness = 1 mm. The other data, for example, functional scan and clinical scans were described in our previous publications [Ji et al., 2013], and did not present in the current work.

Preprocessing

Voxel-based morphometry (VBM) analysis on high-resolution T1-weighted images were processed using VBM8 (<http://dbm.neuro.uni-jena.de/vbm>) implemented in SPM8 (<http://www.fil.ion.ucl.ac.uk/spm>). To increase statistical power, the data of right-side mTLE and the matched HCs were left-right flipped to produce homogenous left-sided dataset [Bonilha et al., 2007; Zhang et al., 2014, 2015]. The images of each subject were then transformed into standard MNI space by normalizing to a symmetric template with a 12-parameter affine-only non-linear transformation, and re-sampled to $1.5 \times 1.5 \times 1.5$ mm³. The symmetric template image was created by averaging the MNI template and its mirror copy reversed in the sagittal plane. All images were segmented into three tissue classes representing GM, WM, and cerebrospinal fluid. The resultant probabilistic GM maps were further smoothed with an 8 mm FWHM isotropic Gaussian kernel for subsequent morphological analyses.

VBM Analysis: Atrophy Patterns and Relevancies with Progressive Factors in mTLE

First, GMV data of patient and HC groups were compared using two-sample t-tests implemented in SPM8 were performed to map the overall GMV alterations in mTLE ($P < 0.01$, FDR correction). Moreover, a lower threshold was used for observing the possible increase of GMV in mTLE ($P < 0.05$, FDR correction). Subsequently, voxel-wise Spearman correlation analysis was performed between GMV data and progressive factors of epilepsy duration and estimated number of seizure events ($P < 0.05$, FDR correction), which aimed to localize the regions showing progressive GMV reduction. Due to the large variance and nonlinearity of data, the variables of estimated number of lifetime seizures were ranked. To maintain consistence, epilepsy durations were also ranked. In the above analyses, the individual gender, age, and lateralization were regressed as covariates.

VBM Analysis: Stage-Specific Atrophy Patterns in mTLE

To map the pattern of progressive GMV alterations in mTLE, we investigated stage-specific GMV reductions in

mTLE. In line with the procedures in the previous works [McDonald et al., 2009; Seeley et al., 2008], we arbitrarily categorized the patients into four subgroups ($n = 27$) from low to high stages of progressive factors (Epilepsy duration: stage I/II/III/IV = 0.5–4.5 years/4.5–11.6 years/11.6–16.5 years/16.6–40 years; Estimated number of lifetime seizures: stage I/II/III/IV = 5–60 times/60–300 times/300–800times/>800 times). GMV data of each subgroup was compared with those of HCs using two-sample *t*-test implemented in SPM8 ($P < 0.01$, *FDR* correction). There was no gender ($\chi^2 = 11.47$, $P = 0.36$; Chi-square analysis) and age ($F = 1.36$, $P = 0.26$; one way-ANOVA) differences among subgroups based on epilepsy duration and HCs. When we grouped the patients based on the estimated number of lifetime seizures, there was no gender difference ($\chi^2 = 11.47$, $P = 0.41$, Chi-square analysis), but mild age difference ($F = 3.57$, $P = 0.04$; one way-ANOVA) among subgroups and HCs. The gender, age, and lateralization were also included as covariates in these analyses.

Hippocampus-Associated SCN for Mapping Synchronized GMV Alterations with Hippocampus

In line with the procedure of the VBM-based SCN computation in the previous work [Bonilha et al., 2007; Liao et al., 2013; Zhang et al., 2011; Zielinski et al., 2010], we constructed SCN by seeding at hippocampus of epileptogenic focus. Seeding region was selected from the hippocampus showing significant GMV reduction (MNI coordinates: $-31, -13, -18$) in the two-sample *t*-test whole group comparison (a critical threshold of $P < 0.00001$ with *FDR* correction was specifically used). In each group of patients and HCs, the averaged GMV values in the seeding region were extracted from each subject and used as a regressor in the General-linear-model in SPM8 to produce VBM-SCN *t*-maps ($P < 0.01$, *FDR* correction). Subsequently, a multi-regression model-based linear-interaction analysis [Bernhardt et al., 2008] was used to detect SCN alteration of the patients relative to the HCs ($P < 0.05$, *FDR* correction within mask of VBM-SCNs combining patients and HCs). The total intracranial volume, individual gender, age, and lateralization were modeled as covariates in regression analyses.

Hippocampus-Associated CaSCN for Mapping Causal Effect of Hippocampal Atrophy on Whole-Brain GMV Alterations in mTLE

According to the ranks of the epilepsy duration and number of seizure events, all the GMV data were sequenced, respectively. The operation of data sequencing granted “time-series” information to the cross-sectional data for describing progressive property of epilepsy. Subsequently, GCA was applied to this “pseudo-time series” data for construct CaSCN seeding at the hippocampus.

Seeding regions of atrophied hippocampus was the same as that in above SCN analysis. The averaged GMV values within the hippocampus were extracted from the sequenced morphological data and constitute a “pseudo-time series”. Signed-path coefficient GCA was voxel-wisely performed in the whole brain using REST-GCA, a plug-in implemented in REST software (<http://www.rest-fmri.net>) [Zang et al., 2012]. GCA was first proposed for determining whether the past value of a time course could correctly predict the current value of another. If the current value of time course Y could be more accurately estimated by the combination of past value of time courses X and Y than the past value of Y alone, then X has Granger causal influence on Y [Granger, 1969]. Accordingly, the CaSCN, by applying GCA to the pseudo-time-series morphometric data through data sequence, could estimate the causal effect of morphometric alteration of a region on the others. Based on the presumption that the hippocampus is the origination of pathological alteration of brain structures in mTLE, we only adopted GC value of X to Y in the current work. To present the GC values with statistical parameters, the original GC map were transformed to z score map [Zang et al., 2012]. The results of CaSCNs were presented using threshold of $P < 0.05$, *FDR* correction.

For further investigate relationships of temporal precedence among these regions one another, we further calculated ROI-based GCA among regions within temporal epileptic network. ROIs were extracted from the results of overall GMV atrophy in two-sample *t*-test group comparison (five ROIs including the hippocampus and lateral temporal cortex ipsilateral to the epileptogenic side, the bilateral prefrontal cortex, thalamus, and cerebellum). Bivariate conditional coefficients GCA was used to construct a network depicting interregional GC relationships among ROIs. Sign-GC values were *t*-distribution transformed in order to assess the statistical significance of the results ($P < 0.05$). In line with the above analysis, only GC values of X to Y were studied.

RESULTS

GM Atrophy Pattern and Correlations with Progressive Factors in mTLE

To evaluate the overall GM atrophy pattern in mTLE, we performed two-sample *t*-test analysis of Gray-matter volume (GMV) generated from voxel-based morphometry. Compared with the HCs, the patients with mTLE showed overall GMV reductions in the mesial and lateral temporal lobes ipsilateral to the epileptogenic side, the bilateral frontal lobes, thalamus, and cerebellum. Moreover, at a lower threshold ($P < 0.05$, *FDR* correction), increased GMV could be found in the contralateral amygdale and posterior cingulate cortex (Fig. 1A). The results also summarized in the Supporting Information Table 1. In the results of correlation analyses between GMVs and progressive

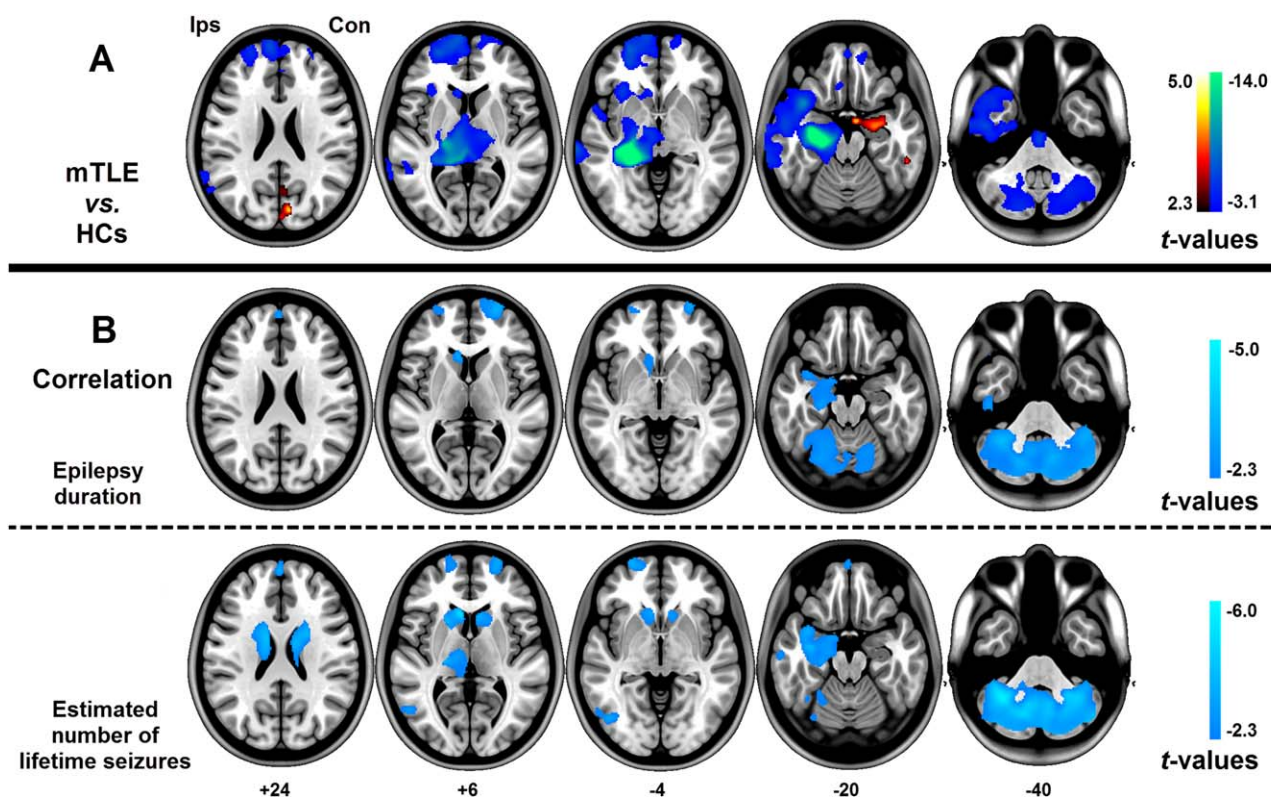


Figure 1.

Gray matter atrophy and its relationships with progressive factors in mTLE. A: Group comparison of GMV between mTLE and healthy controls using two-sample *t*-test ($P < 0.01$, *FDR* correction). Decreased GMV in mTLE was distributed at the mesial and lateral temporal lobes ipsilateral to the epileptogenic side, the bilateral thalamus, frontal lobes and cerebellum. GMV increase was found in the contralateral amygdale and posterior cingulate cortex by lowering threshold ($P < 0.05$, *FDR* correction). B: Correlation analyses between GMV and progressive

factors of epilepsy duration (Upper) and estimated number of lifetime seizures (Lower) in mTLE. For epilepsy durations, negative correlation was found in the ipsilateral hippocampus, bilateral frontal lobe, and cerebellar hemispheres; for number of lifetime seizures, negative correlation was found in the ipsilateral thalamus and bilateral caudate nuclei in addition to the correlation results of epilepsy duration. [Color figure can be viewed at wileyonlinelibrary.com]

factors (Fig. 1B). Longer epilepsy duration or greater number of lifetime seizures was associated with lower GMV in ipsilateral hippocampus, bilateral frontal lobe, and cerebellar hemispheres. In addition, greater number of lifetime seizures was related to lower GMV in the ipsilateral thalamus and bilateral caudate nuclei (Supporting Information Tables 2 and 3).

Stage-Specific GMV Reductions in mTLE

Next, we sought to address whether and how the GMV reductions progressed in stage-specific manner in mTLE. By grouping the patients into four stages according to the progressive factors of epilepsy duration and estimated number of lifetime seizures, we found progressive patterns of reduced GMV in mTLE. With increased epilepsy durations, GMV reductions progressively expanded from the

ipsilateral hippocampus and thalamus (stage I) to the ipsilateral frontal lobe (stages II and III), to the thalamus (stages II, III, and IV), to the cerebellar hemispheres (stages III and IV) and to the bilateral frontal lobe (stage IV) (Fig. 2A). For the number of lifetime seizures, the patterns of progressive GMV reductions were almost similar with those of epilepsy durations, in addition to the bilateral caudate at the stage IV (Fig. 2B). The results were also detailed in the Supporting Information Tables 4 and 5.

Synchronized GMV Alterations with Hippocampal Atrophy Shown by Hippocampus-Associated SCN

We constructed hippocampus-associated SCN by calculating correlation of GMVs between whole brain and the seeding region of hippocampus. In both groups of patients

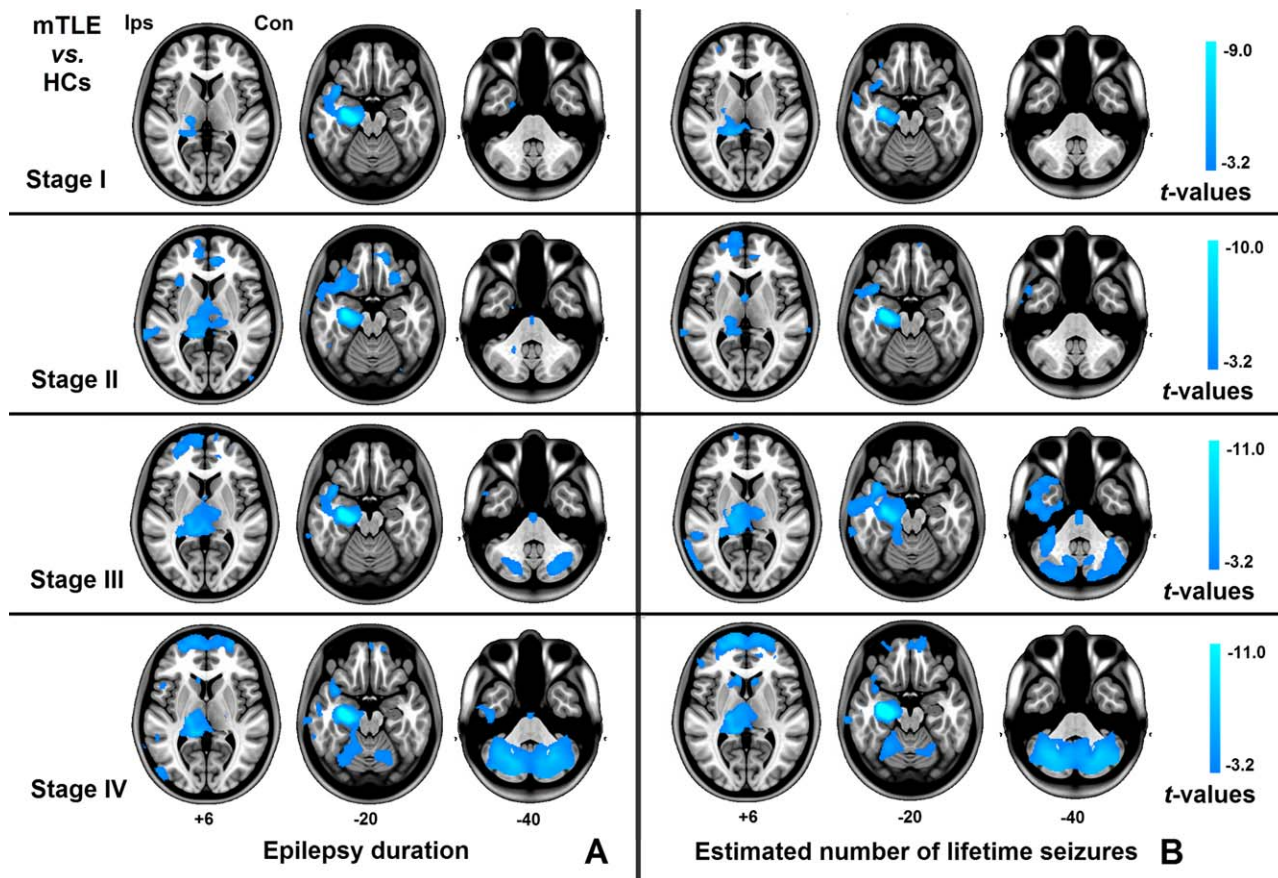


Figure 2.

Progressive patterns of stage-specific GMV alterations in mTLE relative to healthy controls. A: Stages categorized by epilepsy duration (stage I/II/III/IV = 0.5–4.5 years/4.5–11.6 years/11.6–16.5 years/16.6–40 years). With increase of stages, GMV reductions progressively expand from mesial temporal structure to the thalamus, frontal lobe, and cerebellum. B: Stages categorized by

estimated number of lifetime seizures (stage I/II/III/IV = 5–60 times/60–300 times/300–800 times/>800 times). With increase of stages, GMV reductions progressively expand from mesial temporal structure to the lateral temporal lobe, thalamus, frontal lobe, caudate heads, and cerebellum. [Color figure can be viewed at wileyonlinelibrary.com]

(Fig. 3A) and HCs (Fig. 3B), the SCNs showed positive GMV covariance in the ipsilateral temporal cortex, contralateral hippocampus, bilateral thalami, and caudate heads. Compared with the HCs, the patients showed increased connectivity (GMV covariance) in the ipsilateral lateral temporal regions, and decreased connectivity in the ipsilateral lateral temporal cortex and contralateral hippocampus (Fig. 3C). The results were also detailed in the Supporting Information Tables 6–8.

Causal Effect Hippocampal Atrophy on Whole Brain GMV Alterations with Epilepsy Progression Shown by Hippocampus-Associated CaSCN

By applying granger causality analysis to morphometric data sequenced with progressive factors, we constructed

CaSCNs. In the CaSCN based on data sequencing with epilepsy duration (Fig. 4A), the positive values were bilaterally and ipsilaterally located in the lateral temporal lobes, lateral and medial frontal cortices, parietal cortices, thalamus, and cerebellum; the negative regions include the contralateral lateral temporal cortex and bilateral caudate heads, putamen, and posterior-cingulate cortex. In the CaSCN with number of lifetime seizures (Fig. 4B), positive values were ipsilaterally located in the lateral temporal cortex, lateral, and medial frontal cortices and insula, bilaterally located in the putamen, caudate heads, thalamus, and cerebellum; the negative regions include the bilateral posterior cingulate cortex and contralateral temporal cortices (Tables I and II).

ROI-based CaNSC revealed a directional network showing interregional relationship of temporal precedence. In both networks based on data sequencing with epilepsy

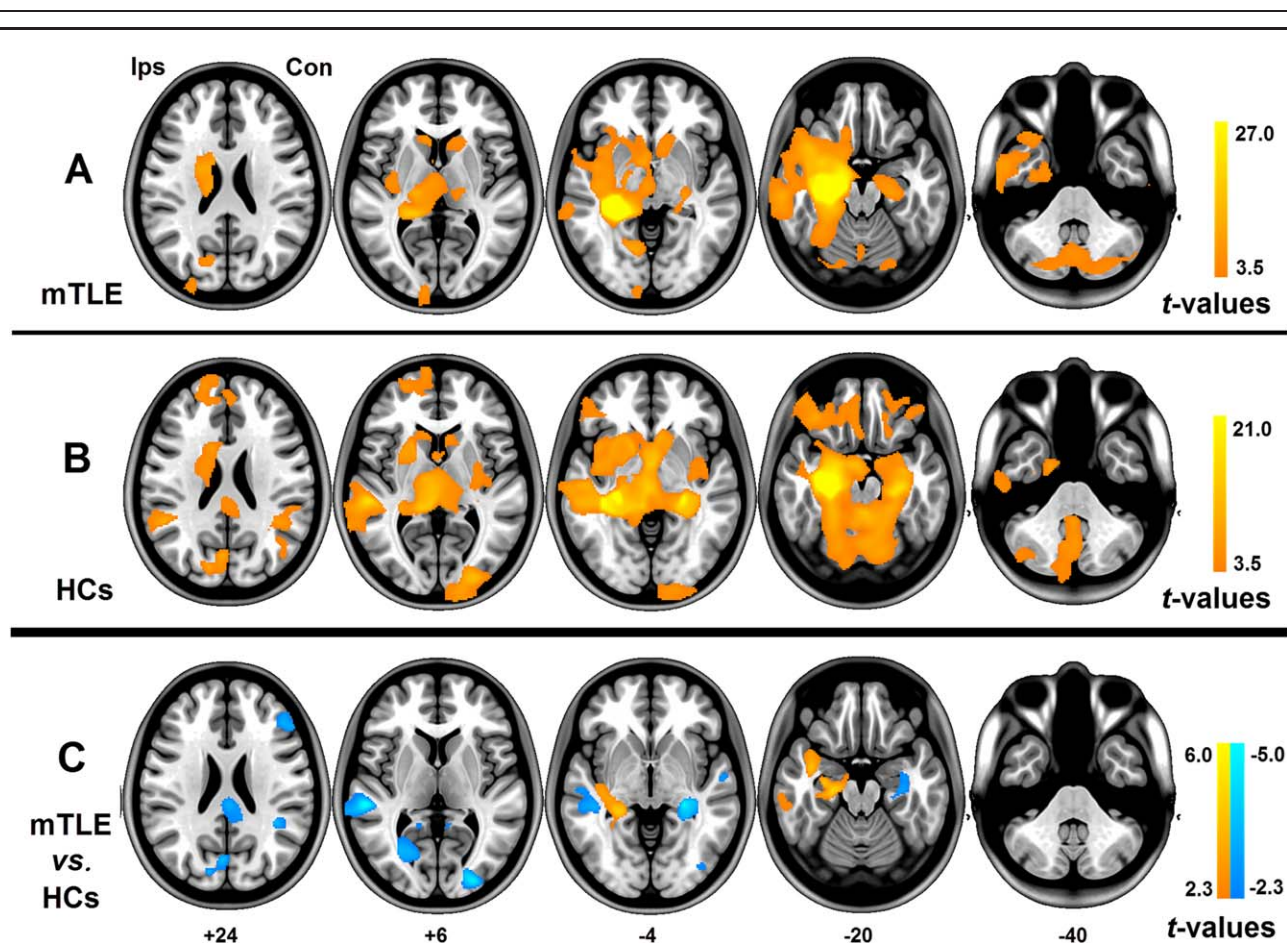


Figure 3.

Patterns of hippocampus-associated structural covariance networks (SCN). A: SCN of mTLE, B: SCN of the healthy controls. Based on a large cohort of cross-sectional morphometric data of patients and controls, SCNs were constructed seeding at the hippocampus showing significant GMV reduction in mTLE. In each group of patients and HCs, the averaged GMV values in the seeding region were extracted from each subject and used as a regressor in the General-linear-model to produce VBM-SCNs of each group. C: Comparison of SCN between patients

with mTLE and healthy controls. Comparing analysis was performed using multi-regression model-based linear-interaction analysis. In the patients with mTLE, increased synchronization of GMV alterations (GMV covariance) with seeding region (hippocampus) was presented in the ipsilateral mesial temporal regions, and decreased synchronization was presented in the ipsilateral lateral temporal cortex and contralateral hippocampus. [Color figure can be viewed at wileyonlinelibrary.com]

duration and number of lifetime seizures, we could find that the hippocampus and the thalamus were prominent node exerting causal effects on other regions, and the pre-frontal cortices and the cerebellum were prominent regions being subject to causal effects from other regions (Fig. 5).

DISCUSSION

By proposing a novel strategy of CaSCN, this work estimated the causal influence of hippocampus on progressive morphometric alterations of epileptic network regions in mTLE. Along with the increases of epilepsy duration and

seizure times, the bilateral frontal and temporal lobes, thalamus, and cerebellum showed consistent positive GC values, and the PCC and contralateral lateral temporal regions showed negative GC values; whereas the basal ganglia including the bilateral caudate heads and putamen showed opposite GC values. The pattern of CaSCN could be partially recapitulated by the stage-specific comparing analysis and SCN analysis.

This work proposed a novel approach of CaSCN by applying GCA to a cohort of cross-sectional morphometric data. Operation of data sequence is the essential for this strategy, which gives “time” property to cross-sectional data. In functional data application, GC connectivity implies that the neuronal activity in region A precedes

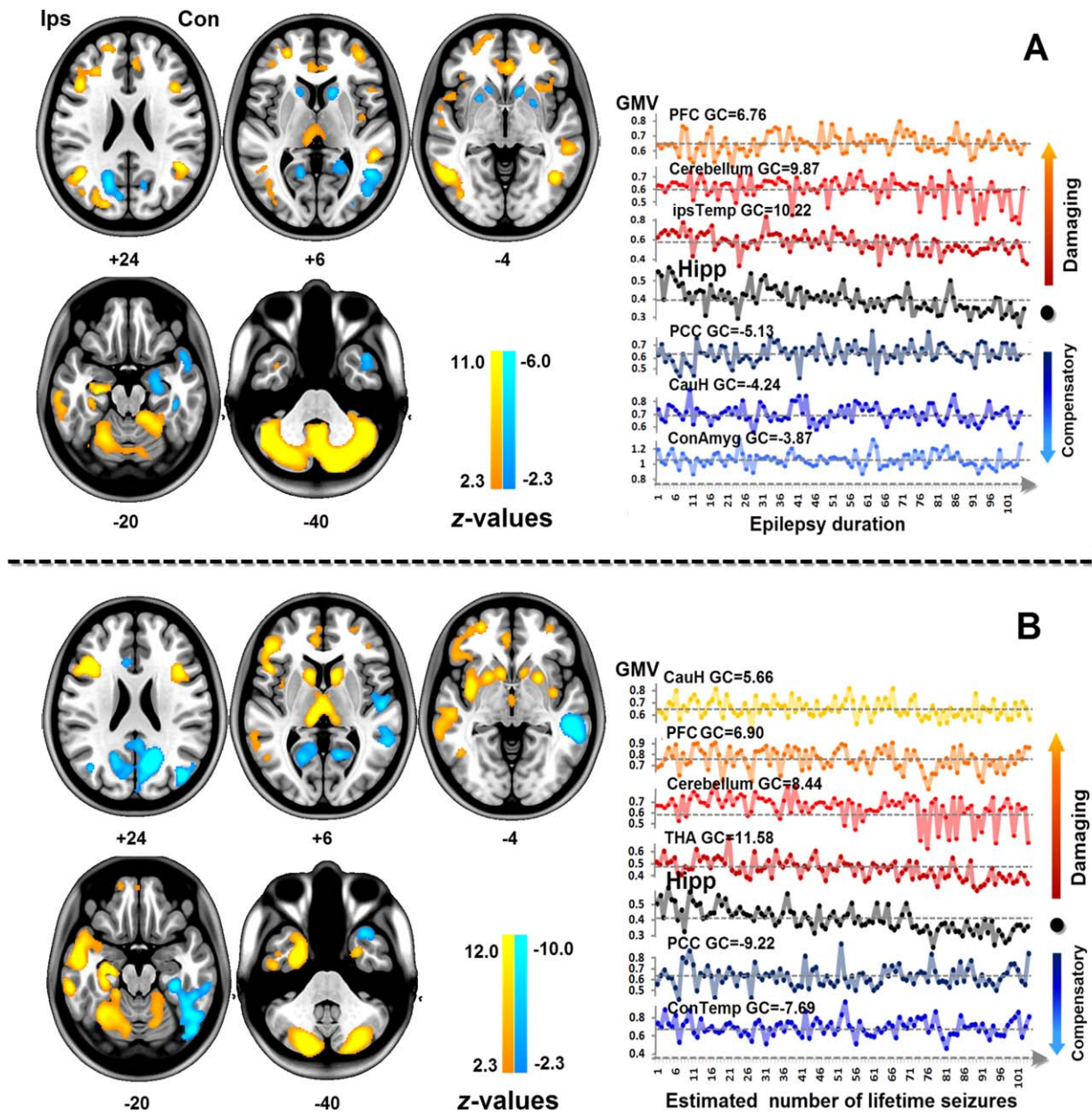


Figure 4.

Hippocampus-associated causal networks of structural covariance (CaSCNs) in mTLE. CaSCNs were constructed by applying granger causal (GC) analysis to a large-cohort of sequenced morphometric data according to progressive factors of epilepsy duration (A) and estimated number of lifetime seizures (B). Seeding region was identical to that in SCN analysis. In both CaSCNs with epilepsy duration and number of lifetime seizures, the lateral temporal lobe ipsilateral to epileptogenic focus, bilateral lateral prefrontal cortices, medial prefrontal cortex and thalamus present consistent positive GC value, the contralateral temporal cortex and posterior-cingulate cortex present consistent negative GC value. The contralateral amygdala shows negative GC value only in the CaSCN with epilepsy duration, and the bilateral insula show positive GC value only in the CaSCN with estimated number of lifetime. The bilateral basal ganglia including the caudate head and

putamen show opposite GC values in these two CaSCNs. The positive GC value denotes that the GMV reduction in the region has causal relationship with, and is preceded by hippocampal atrophy, which may imply seizure damaging effect from hippocampus. The negative GC value denotes that the regions show an opposite (enlarged) GMV alteration caused by hippocampal atrophy, which is explained as compensatory effect of brain structure. The lower figures present causal relationship between hippocampal atrophy and GMV alterations in the other regions within a glass brain. Time series consist of averaged GMV values extracted from the regions showing GC connectivity with hippocampus. X-axis: progressive factors (patients sequenced by progressive factors), Y-axis: GMV values. [Color figure can be viewed at wileyonlinelibrary.com]

TABLE I. Hippocampus-associated causal network of structural covariance with epilepsy duration

Brain regions	MNI coordinates (<i>x,y,z</i>)	GC (z scores)	Number of voxels
ipsLatTemp	-58,-42,-12	10.22	3,903
ips Cerebellum	-18,-67,-54	9.87	15,267
con Cerebellum	33,-61,-55	8.91	13,172
ipsIPL	-43,-61,28	6.79	761
ipsLPFC	-43,21,21	6.76	2,693
conIPL	46,-52,22	6.24	758
conLatTemp	55,-36,0	4.78	1,513
conLPFC	37,49,7	4.62	1,220
Thalamus	-4,-21,6	4.27	529
conTempPole	48,7,-33	-5.98	1,752
PCC	-18,-60,16	-5.13	2,281
conCauH	13,16,3	-4.69	473
conAmyg	25,-12,-19	-3.87	682
ipsCauH	-15,18,1	-3.79	205
ipsPut	-24,9,-3	-3.59	93
conPut	25,6,-6	-3.56	143

Abbreviations: ips-, ipsilateral to the epileptogenic focus; con-, contralateral to the epileptogenic focus; Hipp, Hippocampus; Lat-Temp, lateral temporal cortex; LPFC, lateral prefrontal cortex; MPFC, mesial prefrontal cortex; PCC, posterior cingulate cortex; TempPole, pole of temporal lobe. CauH, Head of caudate; Ins, insular; Put, putamen; IPL, inferior parietal lobular; MNI, Montreal Neurological Institute; GC, granger causality values.

and predicts the neuronal activity that occurs in region B [Goebel et al., 2003; Hamilton et al., 2011; Ji et al., 2013; Palaniyappan et al., 2013]. In analogue, we proposed, the CaSCN may reflect the morphometric alteration in seeding regions precedes and predicts the morphometric alterations that occurs in other network regions along with disease progression. In contrast to other neuroimaging strategies for mapping disease progression, for example, stage-specific comparisons [McDonald et al., 2009; Seeley et al., 2008] and longitude study [Bernhardt et al., 2009, 2013b; Coan et al., 2009; Liu et al., 2001], this CaSCN has advantage on description of network property of involved regions. In contrast to SCN which measuring the synchronization of interregional morphometric alterations [Bernhardt et al., 2008; Bonilha et al., 2007; Zielinski et al., 2010], CaSCN can describe the information of progressive network damage, and importantly, can estimate the causal relationships of interregional structural damages. In the present results, the CaSCN (Fig. 4), rather than the SCN (Fig. 3), could capitulate the spatial pattern of affected regions in mTLE which revealed by comparing (Figs. 1A and 2) and correlation analyses (Fig. 1B). The results imply that CaSCN is more theoretically reasonable and empirically sensitive than SCN to measure the interregional covariance of structural alterations under pathological affection.

Positive GC value was found in the ipsilateral lateral temporal cortex, bilateral frontal cortex, thalamus, and

cerebellum both in the CaSCNs with epilepsy duration and estimated number of lifetime seizures. These structures are essential nodes engaging in propagation and modulation of seizure activity in temporal epilepsy network [Barron et al., 2012, 2014; Blumenfeld et al., 2004; Bonilha et al., 2010; Keller et al., 2014; Spencer, 2002], and are also preferentially damaged regions underlying cognitive impairments in mTLE [Bell et al., 2011; Blumenfeld, 2012; Jokeit et al., 1997]. GMV reduction of these regions has been reported in a large body of literature [Bernasconi et al., 2004; Bernhardt et al., 2013a; Bonilha and Halford 2009; Bonilha et al., 2007; Keller and Roberts 2008; Mueller et al., 2010; Szabo et al., 2006]. Consistent results were also presented in the group comparing analyses in the present work. The positive GC value implied regional GMV reduction succeeding hippocampal atrophy, which could be explained as damaging effect of brain structure caused by seizure activity from hippocampus [Lin et al., 2008; Spencer, 2002]. Alternatively, it is also possible that loss of hippocampal connections leads to remote deafferentation and thereby neuronal damage, particularly for structures directly connected to the hippocampus [Barron et al., 2014; Bonilha et al., 2010]. Moreover, the GC results could also implicate chronological orders of GMV reductions of these regions. With this respect, the presences of the CaSCNs were consistent with progressive GMV reductions revealed by stage-specific comparing analyses (Fig. 2). We could find that the ipsilateral lateral temporal cortex and the

TABLE II. Hippocampus-associated causal network of structural covariance with estimated number of lifetime seizures

Brain regions	MNI coordinates (<i>x,y,z</i>)	GC (z scores)	Number of voxels
Thalamus	-6,-19,7	11.58	1,666
ipsLatTemp	-54,-9,16	8.56	5,760
ips Cerebellum	-16,-85,-37	8.44	7,828
con Cerebellum	37,-64,-52	7.55	7,982
ipsLPFC	-40,24,19	6.90	5,695
ConCauH	12,12,4	6.40	444
IpsIns	-37,-1,-4	6.08	952
conPUT	24,9,-1	5.69	299
ipsCauH	-12,10,7	5.66	762
ipsPUT	-21,10,-6	5.37	720
conLPFC	30,52,1	5.36	339
MPFC	-6,43,1	4.11	1,082
conIPL	36,-34,42	-9.37	1,063
PCC	-16,-60,18	-9.22	2,063
conLatTemp	51,-33,-1	-7.69	3,426

Abbreviations, ips-, ipsilateral to the epileptogenic focus; con-, contralateral to the epileptogenic focus; Hipp, Hippocampus; Lat-Temp, lateral temporal cortex; LPFC, lateral prefrontal cortex; MPFC, mesial prefrontal cortex; PCC, posterior cingulate cortex; TempPole, pole of temporal lobe. CauH, Head of caudate; Ins, insular; Put, putamen; IPL, inferior parietal lobular; MNI, Montreal Neurological Institute; GC, granger causality values.

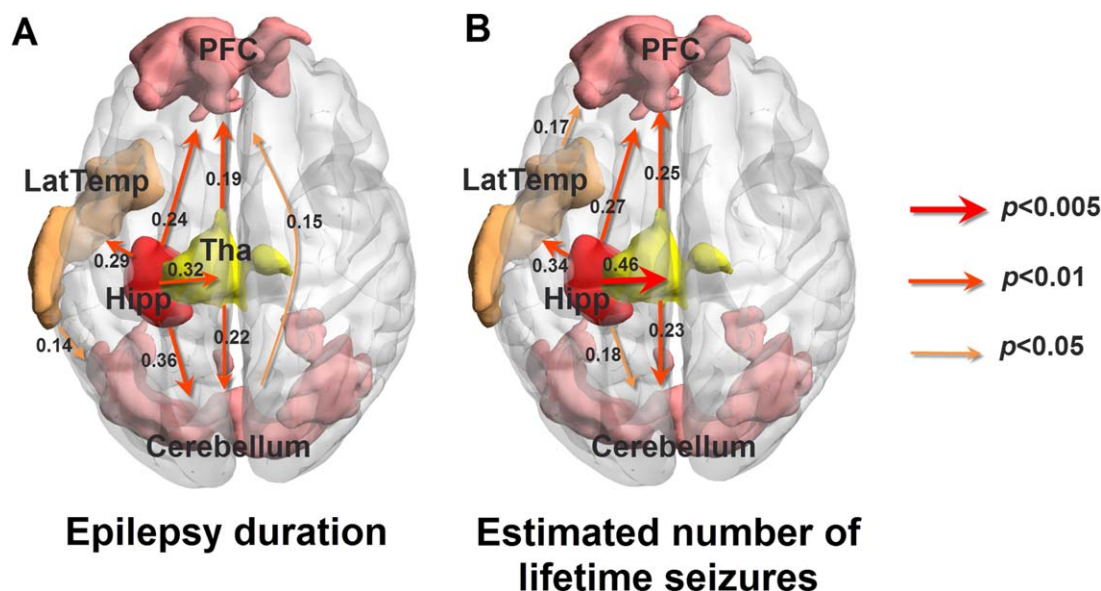


Figure 5.

ROI-based analysis of causal networks of structural covariance. Five ROIs were selected from the results of overall GMV atrophy in two-sample *t*-test group comparisons. In both networks based on data sequencing with epilepsy duration (A) and number of lifetime seizures (B), in addition to the hippocampus, the

thalamus was another prominent node exerting causal effects on other regions, and the prefrontal cortices and the cerebellum were prominent regions being subject to causal effects from other regions. [Color figure can be viewed at wileyonlinelibrary.com]

thalamus presented GMV reductions in the earlier stages (I–II), while the frontal regions and cerebellum presented GMV reductions in the later stages (III–IV) in mTLE. These results might indicate that during pathological process of epileptic seizure damage on brain structures, seizures originate from epileptogenic region (hippocampus), propagate via specific network nodes (e.g., thalamus), and preferentially cause damages of brain regions with different orders [Barron et al., 2012, 2014; Keller et al., 2014]. ROI-based analysis of CaSCN further displayed that the hippocampus and the thalamus were prominent nodes exerting causal effects (i.e., GM reduction) on other regions and that the prefrontal cortex and cerebellum were prominent nodes being subject to causal effects. In summary, the present study clarified the causal relationship of GM atrophy between hippocampus and the other temporal epilepsy network regions, which implicated the significance of early seizure control for mTLE therapy.

Negative GC value was found in the contralateral temporal pole and post-cingulate cortex with both progressions of epilepsy duration and seizures time, and was also found in the contralateral amygdala with progression of seizures time. In GCA study on functional data, a path coefficient of -1 from region X to Y suggests that one unit of change in the activity of region X in a specific direction brings a unit change in the activity of region Y in the opposite direction [Hamilton et al., 2010; Ji et al., 2013; Palaniyappan et al., 2013]. Likewise, the negative GC value in

CaSCN may imply an opposite (enlarged) GMV alteration caused by hippocampal atrophy. There were three types of explanations for our results: firstly, the negative GC value in the contralateral amygdala was interpreted as volumetric enlargement. Enlarged amygdala associated with dysthymia in mTLE has been found in mTLE although divergent alterations were reported in various studies [Bernasconi et al., 2005; Bernhardt et al., 2013b; Coan et al., 2013; Mitsueda-Ono et al., 2011; Takaya et al., 2012; Tebartz van Elst et al., 1999; Van Elst et al., 2000]. Group comparing analysis in the present study also revealed increased GMV of amygdala in mTLE. Importantly, this study for the first time implicate that the enlarged amygdala is causally influenced by hippocampal atrophy in mTLE. Secondly, negative GC in the contralateral temporal lobe and post-cingulate cortex might be speculated as compensatory hypertrophy effect responsible for seizure damage. Increase of GMV in these two regions could be found in group comparing analysis by lowering statistic threshold. Functional compensatory in the contralateral temporal regions in mTLE has been well described in functional imaging studies [Bettus et al., 2009, 2010; Zhang et al., 2010]. Negative GC value in the post-cingulate cortex might be associated with functional and structural alterations in the default brain regions in mTLE [Zhang et al., 2010]. Thirdly, possibility of cell swelling caused by seizures might not be fully excluded [Briellmann et al., 2005].

Epilepsy duration and seizure occurrence are two common factors for describing epilepsy progression, and have been both displayed to associate with progressive structural damage in mTLE [Alhusaini et al., 2012; Bernasconi et al., 2004, 2005; Bonilha et al., 2006; Coan and Cendes 2013; Fuerst et al., 2003; Keller et al., 2002; Liu et al., 2003; Tasch et al., 1999]. The correlation analyses in this study also presented similar patterns of GMV alterations associated with epilepsy duration and seizure number (Fig. 1B). However, in the CaSCN analyses, we could find distinct topological patterns of hippocampus associated CaSCNs using different sequencing ways of epilepsy duration and number of lifetime seizures. This finding suggested that, the CaSCN approach, with temporal information through data sequencing, could more effectively distinguish effects of epilepsy duration and seizure occurrences on GM alterations in mTLE. Epilepsy duration preferentially reflects chronicity, and seizure times more directly reflects damaging severity of epilepsy [Coan and Cendes 2013; Seidenberg et al., 2005]. On the other hand, the finding also indicates that the CaSCN result reflects physiological significance, instead of algorithmic effect in network construction. Specifically, the basal ganglia, including the caudate heads and putamen, showed negative values in the CaSCN with epilepsy duration, and showed opposite positive values in the CaSCN with seizure number. Basal ganglia are considered to be engaged in seizure-modulating and posture seizures in mTLE [Bouilleret et al., 2008; Norden and Blumenfeld 2002]. The opposite GC values in the basal ganglia might imply that these regions presented divergent responses for pathological influences from hippocampus with progressions of epilepsy duration and seizure occurrence. Previous studies have displayed basal ganglia atrophy associated with seizure occurrences [Bouilleret et al., 2008; Szabo et al., 2006]. The correlation (Fig. 3) and stage-specific comparing analyses (Fig. 2) also showed that prominent results in the caudate heads were more associated with factor of seizures number rather than epilepsy duration.

Several methodological limitations of this study should be noted. Firstly, in granger causality analysis, although signal X exerting causal influence on signal Y implies X is preceded by Y, the GC value only implies the extension of causal influence, and cannot directly reflect the quantity of temporal precedence. Although we proposed that CaSCN could reflect both properties of progression and covariance of inter-regional structural damages of epilepsy, longitude analysis of follow-up data [Coan and Cendes, 2013] and network analyses of other imaging modalities [Alexander-Bloch et al., 2013; Evans, 2013] could help to clarify the physiological meaning of CaSCN. Secondly, age effect on CaSCN should be specifically considered in future studies. Thirdly, some clinical variables that might contribute to structural alterations in mTLE were not considered, such as side of seizure focus, initial precipitating index and treatments [Alhusaini et al., 2012; Coan et al., 2009; Coan

and Cendes, 2013]. Moreover, the patient population did not exclusively include drug-refractory cases, whereas broad spectrum of patient types might be more beneficial to the examination of epilepsy progression [Labate et al., 2008]. Fourthly, in the stage-specific comparison analysis, since up to date no standard was available for progression staging of mTLE, four-stages grouping of data in this work was arbitrary. Finally, among clinical variables for describing the progression of epilepsy, we only adopted two common ones: epilepsy duration and estimated number of lifetime seizures. These two variables are time-dependent, but are not real time series. Moreover, pinning down and tracking seizure occurrence was rather difficult, which may ultimately affect the accuracy of these variables.

CONCLUSIONS

We proposed a novel strategy of CaSCN, which allows estimating interregional causal influence of structural alterations with disease progression. Based on this technique, we revealed a hippocampus-associated CaSCN in mTLE consisting of the temporal and frontal cortices, subcortical structures and cerebellum. The hippocampus-associated CaSCN clarified the causal relationship of progressive GM damages between hippocampus and other extra-hippocampal structures in mTLE, indicating damaging and compensatory effects in the extra-hippocampal structures corresponding to hippocampal atrophy in mTLE. Moreover, we observed the different effects of epilepsy duration and seizures occurrence on the trajectory of Gray-matter covariance alternations in mTLE. Our work provided new evidence on the network spread mechanism in terms of the causal influence of hippocampal atrophy on progressive brain structural alterations in mTLE, and had implication for early intervention of epilepsy.

AUTHOR CONTRIBUTIONS

ZZ conceived the work, collected the data, performed the analysis and wrote the manuscript. WL and QX assisted with the analysis of data and generation of the figures. WW, KS and FY assisted with data collections. JZ and DM assisted with manuscript writing and development of the research concept. GL contributed to the development of the research concept.

ACKNOWLEDGMENTS

We thank Prof. Mingzhou Ding, in the department of Biomedical Engineering, University of Florida for his helpful suggestions.

REFERENCES

- Alexander-Bloch A, Giedd JN, Bullmore E (2013): Imaging structural co-variance between human brain regions. *Nat Rev Neurosci* 14:322–336.
- Alhusaini S, Doherty CP, Scanlon C, Ronan L, Maguire S, Borgulya G, Brennan P, Delanty N, Fitzsimons M, Cavalleri GL (2012): A cross-sectional MRI study of brain regional atrophy and clinical characteristics of temporal lobe epilepsy with hippocampal sclerosis. *Epilepsy Res* 99:156–166.
- Barron DS, Fox PM, Laird AR, Robinson JL, Fox PT (2012): Thalamic medial dorsal nucleus atrophy in medial temporal lobe epilepsy: A VBM meta-analysis. *Neuroimage Clin* 2:25–32.
- Barron DS, Tandon N, Lancaster JL, Fox PT (2014): Thalamic structural connectivity in medial temporal lobe epilepsy. *Epilepsia* 55:e50–e55.
- Bartolomei F, Wendling F, Bellanger JJ, Regis J, Chauvel P (2001): Neural networks involving the medial temporal structures in temporal lobe epilepsy. *Clin Neurophysiol* 112:1746–1760.
- Bell B, Lin JJ, Seidenberg M, Hermann B (2011): The neurobiology of cognitive disorders in temporal lobe epilepsy. *Nat Rev Neurol* 7:154–164.
- Berg AT, Scheffer IE (2011): New concepts in classification of the epilepsies: Entering the 21st century. *Epilepsia* 52:1058–1062.
- Bernasconi N, Bernhardt BC (2010): Temporal lobe epilepsy is a progressive disorder. *Nat Rev Neurol* 6:1.
- Bernasconi N, Natsume J, Bernasconi A (2005): Progression in temporal lobe epilepsy: Differential atrophy in mesial temporal structures. *Neurology* 65:223–228.
- Bernasconi N, Duchesne S, Janke A, Lerch J, Collins DL, Bernasconi A (2004): Whole-brain voxel-based statistical analysis of gray matter and white matter in temporal lobe epilepsy. *Neuroimage* 23:717–723.
- Bernhardt BC, Worsley KJ, Besson P, Concha L, Lerch JP, Evans AC, Bernasconi N (2008): Mapping limbic network organization in temporal lobe epilepsy using morphometric correlations: Insights on the relation between mesiotemporal connectivity and cortical atrophy. *Neuroimage* 42:515–524.
- Bernhardt BC, Worsley KJ, Kim H, Evans AC, Bernasconi A, Bernasconi N (2009): Longitudinal and cross-sectional analysis of atrophy in pharmacoresistant temporal lobe epilepsy. *Neurology* 72:1747–1754.
- Bernhardt BC, Hong S, Bernasconi A, Bernasconi N (2013a): Imaging structural and functional brain networks in temporal lobe epilepsy. *Front Hum Neurosci* 7:624.
- Bernhardt BC, Kim H, Bernasconi N (2013b): Patterns of subregional mesiotemporal disease progression in temporal lobe epilepsy. *Neurology* 81:1840–1847.
- Bettus G, Guedj E, Joyeux F, Confort-Gouny S, Soulier E, Laguitton V, Cozzzone PJ, Chauvel P, Ranjeva JP, Bartolomei F, and others. (2009): Decreased basal fMRI functional connectivity in epileptogenic networks and contralateral compensatory mechanisms. *Hum Brain Mapp* 30:1580–1591.
- Bettus G, Bartolomei F, Confort-Gouny S, Guedj E, Chauvel P, Cozzzone PJ, Ranjeva JP, Guye M (2010): Role of resting state functional connectivity MRI in presurgical investigation of mesial temporal lobe epilepsy. *J Neurol Neurosurg Psychiatry* 81:1147–1154.
- Blumenfeld H (2012): Impaired consciousness in epilepsy. *Lancet Neurol* 11:814–826.
- Blumenfeld H, McNally KA, Vanderhill SD, Paige AL, Chung R, Davis K, Norden AD, Stokking R, Studholme C, Novotny EJ, Jr, and others. (2004): Positive and negative network correlations in temporal lobe epilepsy. *Cereb Cortex* 14:892–902.
- Bonilha L, Halford JJ (2009): Network atrophy in temporal lobe epilepsy: A voxel-based morphometry study. *Neurology* 72:2052; author reply 2052.
- Bonilha L, Kobayashi E, Rorden C, Cendes F, Li LM (2003): Medial temporal lobe atrophy in patients with refractory temporal lobe epilepsy. *J Neurol Neurosurg Psychiatry* 74:1627–1630.
- Bonilha L, Rorden C, Appenzeller S, Coan AC, Cendes F, Li LM (2006): Gray matter atrophy associated with duration of temporal lobe epilepsy. *Neuroimage* 32:1070–1079.
- Bonilha L, Rorden C, Halford JJ, Eckert M, Appenzeller S, Cendes F, Li LM (2007): Asymmetrical extra-hippocampal gray matter loss related to hippocampal atrophy in patients with medial temporal lobe epilepsy. *J Neurol Neurosurg Psychiatry* 78:286–294.
- Bonilha L, Edwards JC, Kinsman SL, Morgan PS, Fridriksson J, Rorden C, Rumboldt Z, Roberts DR, Eckert MA, Halford JJ (2010): Extrahippocampal gray matter loss and hippocampal deafferentation in patients with temporal lobe epilepsy. *Epilepsia* 51:519–528.
- Bouillere V, Semah F, Chassoux F, Mantzarides M, Biraben A, Trebossen R, Ribeiro MJ (2008): Basal ganglia involvement in temporal lobe epilepsy: A functional and morphologic study. *Neurology* 70:177–184.
- Briellmann RS, Berkovic SF, Syngeniotis A, King MA, Jackson GD (2002): Seizure-associated hippocampal volume loss: A longitudinal magnetic resonance study of temporal lobe epilepsy. *Ann Neurol* 51:641–644.
- Briellmann RS, Wellard RM, Jackson GD (2005): Seizure-associated abnormalities in epilepsy: Evidence from MR imaging. *Epilepsia* 46:760–766.
- Coan AC, Cendes F (2013): Epilepsy as progressive disorders: What is the evidence that can guide our clinical decisions and how can neuroimaging help?. *Epilepsy Behav* 26:313–321.
- Coan AC, Appenzeller S, Bonilha L, Li LM, Cendes F (2009): Seizure frequency and lateralization affect progression of atrophy in temporal lobe epilepsy. *Neurology* 73:834–842.
- Coan AC, Morita ME, Campos BM, Bergo FP, Kubota BY, Cendes F (2013): Amygdala enlargement occurs in patients with mesial temporal lobe epilepsy and hippocampal sclerosis with early epilepsy onset. *Epilepsy Behav* 29:390–394.
- Duzel E, Schiltz K, Solbach T, Peschel T, Baldeweg T, Kaufmann J, Szentkuti A, Heinze HJ (2006): Hippocampal atrophy in temporal lobe epilepsy is correlated with limbic systems atrophy. *J Neurol* 253:294–300.
- Evans AC (2013): Networks of anatomical covariance. *Neuroimage* 80:489–504.
- Fuerst D, Shah J, Shah A, Watson C (2003): Hippocampal sclerosis is a progressive disorder: A longitudinal volumetric MRI study. *Ann Neurol* 53:413–416.
- Garcia-Finana M, Denby CE, Keller SS, Wieshmann UC, Roberts N (2006): Degree of hippocampal atrophy is related to side of seizure onset in temporal lobe epilepsy. *AJNR Am J Neuroradiol* 27:1046–1052.
- Goebel R, Roebroeck A, Kim DS, Formisano E (2003): Investigating directed cortical interactions in time-resolved fMRI data using vector autoregressive modeling and Granger causality mapping. *Magn Reson Imaging* 21:1251–1261.
- Goncalves Pereira PM, Insausti R, Artacho-Perula E, Salmenpera T, Kalviainen R, Pitkanen A (2005): MR volumetric analysis of

- the piriform cortex and cortical amygdala in drug-refractory temporal lobe epilepsy. *AJNR Am J Neuroradiol* 26:319–332.
- Granger CWJ (1969): Investigating causal relations by econometric models and cross-spectral methods. *Econometrica* 37:424–438.
- Hamilton JP, Chen G, Thomason ME, Schwartz ME, Gotlib IH (2010): Investigating neural primacy in Major Depressive Disorder: Multivariate Granger causality analysis of resting-state fMRI time-series data. *Mol Psychiatry* 16:763–772.
- Hamilton JP, Chen G, Thomason ME, Schwartz ME, Gotlib IH (2011): Investigating neural primacy in Major Depressive Disorder: Multivariate Granger causality analysis of resting-state fMRI time-series data. *Mol Psychiatry* 16:763–772.
- Ji GJ, Zhang Z, Zhang H, Wang J, Liu DQ, Zang YF, Liao W, Lu G (2013): Disrupted causal connectivity in mesial temporal lobe epilepsy. *PLoS One* 8:e63183.
- Jiao Q, Lu G, Zhang Z, Zhong Y, Wang Z, Guo Y, Li K, Ding M, Liu Y (2011): Granger causal influence predicts BOLD activity levels in the default mode network. *Hum Brain Mapp* 32:154–161.
- Jokeit H, Seitz RJ, Markowitsch HJ, Neumann N, Witte OW, Ebner A (1997): Prefrontal asymmetric interictal glucose hypometabolism and cognitive impairment in patients with temporal lobe epilepsy. *Brain* 120 (Pt 12):2283–2294.
- Kalviainen R, Salmenperä T, Partanen K, Vainio P, Riekkinen P, Pitkanen A (1998): Recurrent seizures may cause hippocampal damage in temporal lobe epilepsy. *Neurology* 50:1377–1382.
- Keller SS, Roberts N (2008): Voxel-based morphometry of temporal lobe epilepsy: An introduction and review of the literature. *Epilepsia* 49:741–757.
- Keller SS, Wiesmann UC, Mackay CE, Denby CE, Webb J, Roberts N (2002): Voxel based morphometry of grey matter abnormalities in patients with medically intractable temporal lobe epilepsy: Effects of side of seizure onset and epilepsy duration. *J Neurol Neurosurg Psychiatry* 73:648–655.
- Keller SS, O’Muircheartaigh J, Traynor C, Towgood K, Barker GJ, Richardson MP (2014): Thalamotemporal impairment in temporal lobe epilepsy: A combined MRI analysis of structure, integrity, and connectivity. *Epilepsia* 55:306–315.
- Labate A, Cerasa A, Gambardella A, Aguglia U, Quattrone A (2008): Hippocampal and thalamic atrophy in mild temporal lobe epilepsy: A VBM study. *Neurology* 71:1094–1101.
- Liao W, Zhang Z, Mantini D, Xu Q, Wang Z, Chen G, Jiao Q, Zang YF, Lu G (2013): Relationship between large-scale functional and structural covariance networks in idiopathic generalized epilepsy. *Brain Connect* 3:240–254.
- Lin JJ, Riley JD, Juranek J, Cramer SC (2008): Vulnerability of the frontal-temporal connections in temporal lobe epilepsy. *Epilepsy Res* 82:162–170.
- Liu RS, Lemieux L, Bell GS, Bartlett PA, Sander JW, Sisodiya SM, Shorvon SD, Duncan JS (2001): A longitudinal quantitative MRI study of community-based patients with chronic epilepsy and newly diagnosed seizures: Methodology and preliminary findings. *Neuroimage* 14:231–243.
- Liu RS, Lemieux L, Bell GS, Hammers A, Sisodiya SM, Bartlett PA, Shorvon SD, Sander JW, Duncan JS (2003): Progressive neocortical damage in epilepsy. *Ann Neurol* 53:312–324.
- McDonald CR, McEvoy LK, Gharapetian L, Fennema-Notestine C, Hagler DJ, Jr., Holland D, Koyama A, Brewer JB, Dale AM (2009): Regional rates of neocortical atrophy from normal aging to early Alzheimer disease. *Neurology* 73:457–465.
- Mitsueda-Ono T, Ikeda A, Inouchi M, Takaya S, Matsumoto R, Hanakawa T, Sawamoto N, Mikuni N, Fukuyama H, Takahashi R (2011): Amygdala enlargement in patients with temporal lobe epilepsy. *J Neurol Neurosurg Psychiatry* 82:652–657.
- Moran NF, Lemieux L, Kitchen ND, Fish DR, Shorvon SD (2001): Extrahippocampal temporal lobe atrophy in temporal lobe epilepsy and mesial temporal sclerosis. *Brain* 124:167–175.
- Mueller SG, Laxer KD, Barakos J, Cheong I, Finlay D, Garcia P, Cardenas-Nicolson V, Weiner MW (2010): Involvement of the thalamocortical network in TLE with and without mesiotemporal sclerosis. *Epilepsia* 51:1436–1445.
- Norden AD, Blumenfeld H (2002): The role of subcortical structures in human epilepsy. *Epilepsy Behav* 3:219–231.
- Palaniyappan L, Simmonite M, White TP, Liddle EB, Liddle PF (2013): Neural primacy of the salience processing system in schizophrenia. *Neuron* 79:814–828.
- Pitkanen A, Sutula TP (2002): Is epilepsy a progressive disorder? Prospects for new therapeutic approaches in temporal-lobe epilepsy. *Lancet Neurol* 1:173–181.
- Seeley WW, Crawford R, Rascofsky K, Kramer JH, Weiner M, Miller BL, Gorno-Tempini ML (2008): Frontal paralimbic network atrophy in very mild behavioral variant frontotemporal dementia. *Arch Neurol* 65:249–255.
- Seeley WW, Crawford RK, Zhou J, Miller BL, Greicius MD (2009): Neurodegenerative diseases target large-scale human brain networks. *Neuron* 62:42–52.
- Seidenberg M, Kelly KG, Parrish J, Geary E, Dow C, Rutecki P, Hermann B (2005): Ipsilateral and contralateral MRI volumetric abnormalities in chronic unilateral temporal lobe epilepsy and their clinical correlates. *Epilepsia* 46:420–430.
- Seth AK, Barrett AB, Barnett L (2015): Granger causality analysis in neuroscience and neuroimaging. *J Neurosci* 35:3293–3297.
- Sloviter RS (1999): Status epilepticus-induced neuronal injury and network reorganization. *Epilepsia* 40 Suppl 1:S34–S39.
- Spencer SS (2002): Neural networks in human epilepsy: Evidence of and implications for treatment. *Epilepsia* 43:219–227.
- Szabo CA, Lancaster JL, Lee S, Xiong JH, Cook C, Mayes BN, Fox PT (2006): MR imaging volumetry of subcortical structures and cerebellar hemispheres in temporal lobe epilepsy. *AJNR Am J Neuroradiol* 27:2155–2160.
- Takaya S, Ikeda A, Mitsueda-Ono T, Matsumoto R, Inouchi M, Namiki C, Oishi N, Mikuni N, Ishizu K, Takahashi R, and others. (2012): Temporal lobe epilepsy with amygdala enlargement: A morphologic and functional study. *J Neuroimaging* 24:54–62.
- Tasch E, Cendes F, Li LM, Dubeau F, Andermann F, Arnold DL (1999): Neuroimaging evidence of progressive neuronal loss and dysfunction in temporal lobe epilepsy. *Ann Neurol* 45:568–576.
- Tebartz van Elst L, Woermann FG, Lemieux L, Trimble MR (1999): Amygdala enlargement in dysthymia—a volumetric study of patients with temporal lobe epilepsy. *Biol Psychiatry* 46:1614–1623.
- Van Elst LT, Woermann FG, Lemieux L, Thompson PJ, Trimble MR (2000): Affective aggression in patients with temporal lobe epilepsy: A quantitative MRI study of the amygdala. *Brain* 123 (Pt 2):234–243.
- Wei W, Zhang Z, Xu Q, Yang F, Sun K, Lu G (2016): More severe extratemporal damages in mesial temporal lobe epilepsy with hippocampal sclerosis than that with other lesions: A multimodality MRI study. *Medicine (Baltimore)* 95:e3020.
- Wu JW, Song ZQ, Chen JK, Tan QF, Li SJ, Lu GM, Zhang ZJ, Liu YX (1998): Volumetric measurement of hippocampal formation

- using MRI in the normal Chinese adults and patients with epilepsy. *Chin J Radiol* 32:220–227. (Article in Chinese).
- Zang ZX, Yan CG, Dong ZY, Huang J, Zang YF (2012): Granger causality analysis implementation on MATLAB: A graphic user interface toolkit for fMRI data processing. *J Neurosci Methods* 203:418–426.
- Zhang Z, Lu G, Zhong Y, Tan Q, Liao W, Wang Z, Li K, Chen H, Liu Y (2010): Altered spontaneous neuronal activity of the default-mode network in mesial temporal lobe epilepsy. *Brain Res* 1323:152–160.
- Zhang Z, Liao W, Zuo XN, Wang Z, Yuan C, Jiao Q, Chen H, Biswal BB, Lu G, Liu Y (2011): Resting-state brain organization revealed by functional covariance networks. *PLoS One* 6:e28817.
- Zhang Z, Liao W, Bernhardt B, Wang Z, Sun K, Yang F, Liu Y, Lu G (2014): Brain iron redistribution in mesial temporal lobe epilepsy: A susceptibility-weighted magnetic resonance imaging study. *BMC Neurosci* 15:117.
- Zhang Z, Xu Q, Liao W, Wang Z, Li Q, Yang F, Liu Y, Lu G (2015): Pathological uncoupling between amplitude and connectivity of brain fluctuations in epilepsy. *Hum Brain Mapp* 36:2756–2766.
- Zielinski BA, Gennatas ED, Zhou J, Seeley WW (2010): Network-level structural covariance in the developing brain. *Proc Natl Acad Sci U S A* 107:18191–18196.